AGU ADVANCING EARTH AND SPACE SCIENCE

Water Resources Research®

RESEARCH ARTICLE
10.1029/2021WR030238

Influence of Land Reclamation on Fresh Groundwater Lenses in Oceanic Islands: Laboratory and Numerical Validation

Chong Sheng[1], Jiu Jimmy Jiao[1], Hehua Xu[2,3], Yi Liu[1], and Xin Luo[1]

[1]Department of Earth Sciences, The University of Hong Kong, Hong Kong, China, [2]Key Laboratory of Ocean and Marginal Sea Geology, South China Sea Institute of Oceanology, Innovation Academy of South China Sea Ecology and Environmental Engineering, Chinese Academy of Sciences, Guangzhou, China, [3]Southern Marine Science and Engineering Guangdong Laboratory (Guangzhou), Guangzhou, China

Abstract Fresh groundwater lenses in tropic oceanic islands are important freshwater resources for local inhabitants and ecosystems. These reef-carbonate islands typically have a dual-aquifer structure, with poorly consolidated Holocene sediments deposited unconformably on Pleistocene limestone reef deposits. Land reclamation has been carried out on the reef flats or shallow water areas in coral islands, a very common practice in the Indian Ocean and the South China Sea. However, there is a lack of comprehensive understanding of how the groundwater system will respond to land reclamation. In this study, the impact of land reclamation on the fresh groundwater lens in an island is investigated using multiple methods: sand-tank experiments, sharp-interface analytical solutions, and numerical modeling. This study demonstrates that land reclamation can increase the freshwater storage of the lens and shift the water divide toward the reclamation area. Furthermore, a lower permeability fill material especially with a greater scale or thickness leads to higher freshwater storage. However, the expansion of the lens will be truncated due to the high-permeability of the lower layer. These observations and findings from the laboratory experiments and two-dimensional numerical simulations are further ground-truthed by the three-dimensional modeling of Yongxing Island in the South China Sea. The findings of this study provide a comprehensive understanding of the impact of land reclamation on island groundwater system and the theoretical supports for Small Island Developing States to use the reclamation not only for urban development but also for extra aquifer to enhance the water resource sustainability under the climate change.

Plain Language Summary Groundwater on oceanic islands in the form of fresh groundwater lenses (FGL) that serve as an important freshwater resource for human consumption and ecosystem services. With intensifying sea-level rise and global warming, many oceanic islands are shrinking, which leads to the decreasing or even disappearance of the FGL. Land reclamation seems to be the best choice to provide not only valuable land for urban development, but also extra aquifer space for the storage of freshwater resources. In this research, we evaluated the impacts of land reclamation on FGL by using multiple methods: laboratory sand-tank experiments, analytical solutions, and numerical modeling. Our results show that land reclamation can increase the freshwater storage of the lens and reshape the groundwater system in oceanic islands. Furthermore, a lower permeability fill material especially with a greater scale or thickness leads to higher freshwater storage. However, the expansion of the lens will be truncated due to the high-permeability of the lower layer on tropical coral islands. Finally, these findings above are also further ground-truthed by the three-dimensional modeling of Yongxing Island. Overall, the findings of this work have important global implications for water resources management especially for the Small Island Developing States.

Key Points:

- The impact of land reclamation on the fresh groundwater lens in island was investigated by laboratory, analytical and numerical methods
- Land reclamation increases the fresh groundwater storage and reshapes the groundwater system in the oceanic island
- The response of the fresh groundwater lens to land reclamation in islands is subject to the oceanic aquifer structure

Supporting Information:

Supporting Information may be found in the online version of this article.

Correspondence to:

H. Xu,
xhhcn@scsio.ac.cn

Citation:

Sheng, C., Jiao, J. J., Xu, H., Liu, Y., & Luo, X. (2021). Influence of land reclamation on fresh groundwater lenses in oceanic islands: Laboratory and numerical validation. *Water Resources Research*, *57*, e2021WR030238. https://doi.org/10.1029/2021WR030238

Received 22 APR 2021
Accepted 30 AUG 2021

1. Introduction

There are approximately 425 atolls in the world (Falkland, 1992) and most of them belong to Small Island Developing States (SIDS) in the Indian and Pacific Oceans. About 65 million people live in these SIDS (UN-OHRLLS, 2015). When precipitation recharge across an oceanic island is sufficient, a fresh groundwater lens (or freshwater lens) develops above the denser saline groundwater derived from the sea, which is a

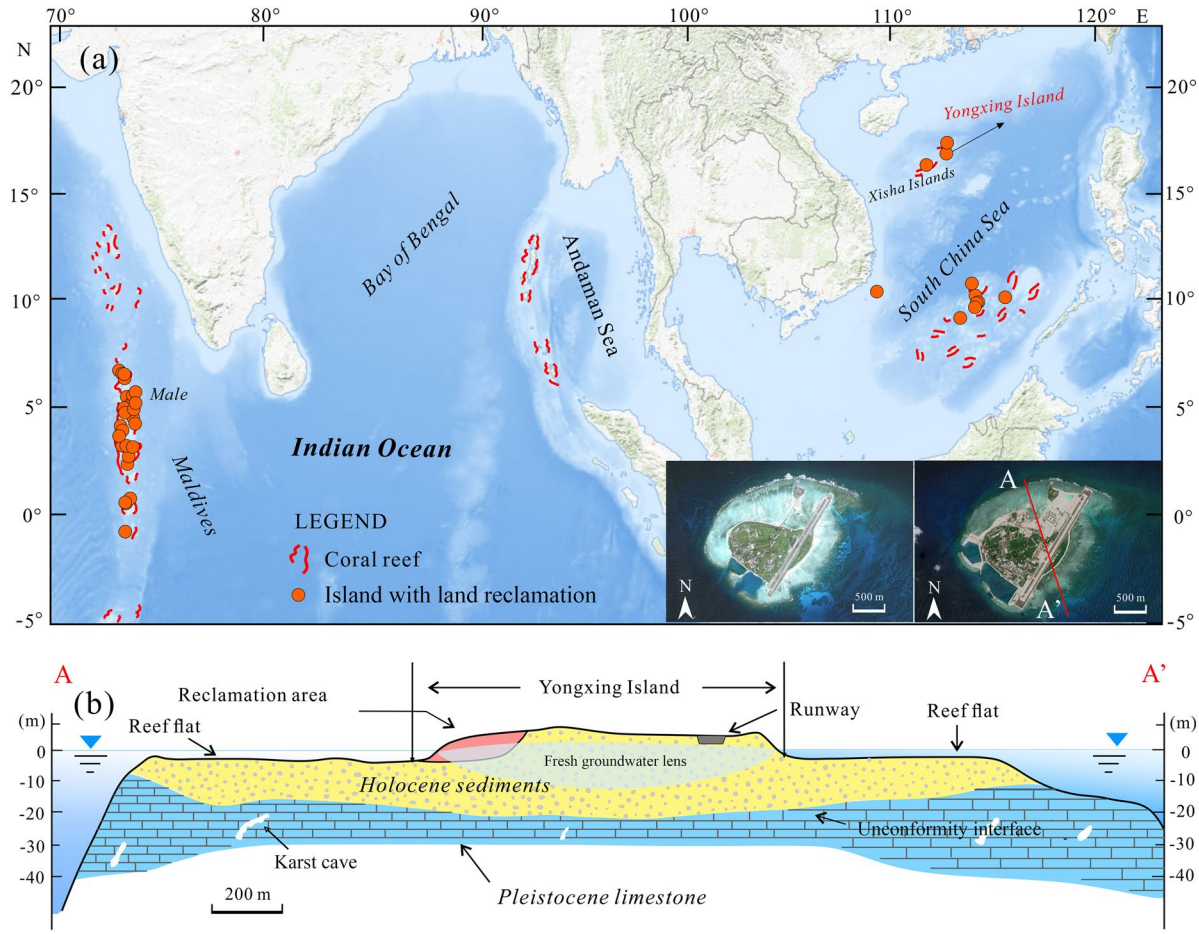

Figure 1. (a) Map of the islands with land reclamation in the South China Sea and Northern Indian Ocean. The insets in (a) are images of Yongxing Island before and after land reclamation. (b) The hydrogeologic profile A-A'of Yongxing Island, which is a typical profile of the atoll island with land reclamation.

common phenomenon observed worldwide (Werner et al., 2017). On inhabited islands, fresh groundwater lens is an important freshwater resource for human consumption and ecosystem services. However, the fresh groundwater lens is highly vulnerable to salinization due to natural recharge variations (Chui & Terry, 2012; Holding & Allen, 2015), inundations (e.g., tsunamis, storm surges, etc.) (Guimond & Michael, 2021), groundwater over-abstraction (Post et al., 2018), and other anthropogenic activities (Bailey & Jenson, 2014; Cozzolino et al., 2017).

According to a field survey undertaken in the South Cocos (Keeling) atolls in the Indian Ocean (Falkland, 1994), under a rainfall of 1,938 mm/y, the threshold width of an island to form a fresh groundwater lens is ~270 m. Thus, the precipitation will rapidly discharge to the ocean and a fresh groundwater lens is not prone to be developed if the island width is less than this threshold width. With intensifying sea-level rise and global warming, many oceanic islands are shrinking, which leads to the shrinking or even disappearance of the fresh groundwater lens (Gulley et al., 2016). To relieve the abovementioned crisis, land reclamation has been carried out in many SIDS (Figure 1, see Supporting Information), such as the Maldive Islands and some islands in the Pacific Ocean. For these islands, large cutter suction dredgers are usually used to cut and pump loose coral gravel excavated in the surrounding lagoon or other parts of the reef and fill or accumulate on the objective reef flat through a duct to form a foundation platform (Sheng et al., 2020). Land reclamation provides not only valuable land for urban development (e.g., Velana International Airport of Maldive) but also extra aquifer space for storage of freshwater resources, as firstly pointed out by Guo and Jiao (2007) and further discussed by other studies (e.g., Jiao & Post, 2019; Lu et al., 2019; Sheng et al., 2017; Yao et al., 2019).

The topographic changes of islands in the natural environment are slow, but land reclamation reshapes the topography of an island within a very short time. Due to the high value of island fresh groundwater lens as an accessible freshwater resource and its vulnerability to environmental variations, some studies have been carried out to delineate the fresh groundwater lens and evaluate its storage for inhabited oceanic islands. The impacts of geological heterogeneity (Schneider & Kruse, 2003), spatial variability of groundwater recharge (Gulley et al., 2016; Tang et al., 2021), storm surge (Chui & Terry, 2013; Gingerich et al., 2017), and sea-level rise (Storlazzi et al., 2018) on the geometry of the fresh groundwater lens have been investigated. Comparatively, much fewer studies have been carried out on the impact of land reclamation on the fresh groundwater lens in a real tropical coral island of multi-layered aquifer structure. Nevertheless, some previous studies show that there is a close relationship between the island geomorphology and the fresh groundwater lens. Röper et al. (2013) studied the development of dunes and accompanying freshwater reservoirs below a former sand plate forming the eastern part of the Spiekeroog Island (northwest of Germany) over the last century through the georeferenced aerial photographs with the density-dependent groundwater flow simulation software SEAWAT, and found that the geometry of the fresh groundwater lens varies with the shape of the island. Besides, the reclamation areas also have the potential as extra aquifer space for the storage of freshwater resources. Yao et al. (2019) used a series of numerical models to quantify the potential maximum storage and formation time of the fresh groundwater lens that can occur in a reclaimed generic island. The results pointed out that most of the total aquifer volume in the reclaimed islands would be replenished with fresh water under an annual recharge rate of 1,000 mm/y within 100 years. Sheng et al. (2020) evaluated the dynamic mechanisms and formation process of the fresh groundwater lens with a typical cross-section in an island with land reclamation in the South China Sea. However, most of those studies emphasized the processes of the fresh groundwater lens from the saltwater to freshwater in a new island entirely reclaimed from the sea. The objective of this study is to explore the impact of land reclamation on the groundwater system in an existing oceanic island that has already formed a fresh groundwater lens, which is the typical situation in the islands experiencing land reclamation in the Indian oceans and South China Sea.

Previous studies have also used different methods to characterize the fresh groundwater lens in oceanic islands. The study by Fetter (1972) provided a general analytical solution to determine the depth of the fresh-saline water interface for homogeneous oceanic islands. Afterward, Vacher (1988) extended Fetter's (1972) results by deriving analytical solutions for infinite strip islands composed of layers of different hydraulic conductivities (K) to describe the lens shape. In recent years, the hydrogeological research group at the University of Hong Kong has carried out a series of studies on the impact of land reclamation on groundwater flows systems. For example, Guo and Jiao (2007) derived analytical solutions with steady-state to demonstrate how the water level and fresh-saline water interface would change with land reclamation along the coast. Hu et al. (2008) derived analytical solutions to study the transient groundwater flow induced by land reclamation. Hu and Jiao (2014) derived analytical solutions to study the response of the groundwater flow to the multiple stages of reclamation using different fill materials. Physical models remain important tools to gain information about fresh and saltwater interaction and the effects of groundwater extraction by wells on the interface (Stoeckl & Houben, 2012). For example, Stoeckl et al. (2015) used a series of sand-tank experiments to study the formation of fresh groundwater lens in heterogeneous aquifers, together with the groundwater flow path and the spatial distribution of groundwater age. Using two-dimensional experiments, Werner et al. (2009) studied the up-coning effects of saltwater plumes and compared their experimental results with a sharp-interface analytical solution. Memari et al. (2020) used a novel radial flow experimental system (three-dimensional) to study the saltwater intrusion in a circular island aquifer. Recently, to explore the methods of increasing fresh groundwater storage of oceanic islands, Lu et al. (2019) presented a sand-tank laboratory experiment combined with analytical solutions to investigate the impact of the less permeable slice along the shoreline of an oceanic island on the fresh groundwater lens. Besides, different types of finite element and finite difference modeling codes have also been used to solve a variety of complex field-scale problems. For example, SEAWAT, a finite difference model developed by the USGS which combines MODFLOW and MT3DMS to simulate variable-density groundwater flow and solute transport and has been also used widely for simulating seawater intrusion in coastal areas (Langevin, 2008). Werner et al. (2017) presented an excellent summary of various numerical methods that were used to study the fresh groundwater lens in oceanic islands.

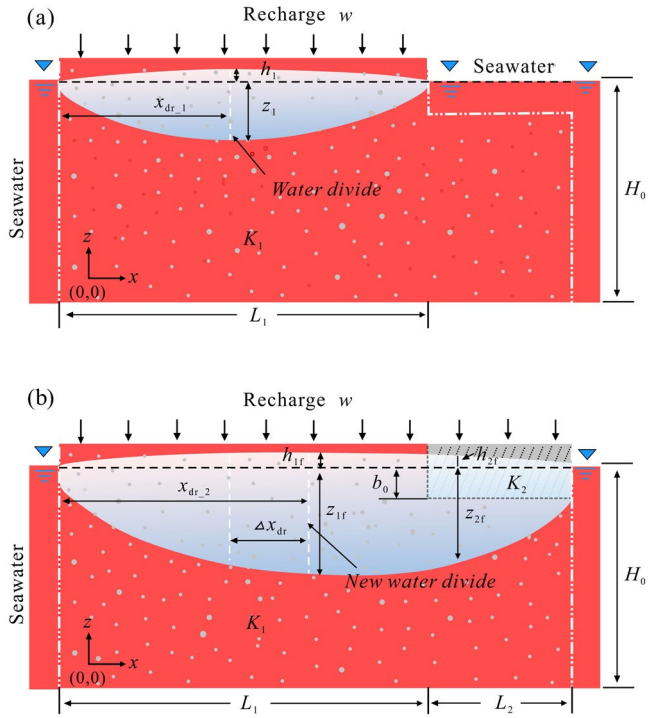

Figure 2. Conceptual models of fresh groundwater lens in an oceanic island before (a) and after (b) land reclamation. The origin ($x = 0$) of the coordinate system is located in the bottom left corner.

Land reclamation usually takes place on the reef flats or other shallow water areas around the tropical islands in the Indian Ocean and the Western Pacific Ocean (see Supporting Information), but so far there have been very limited studies to address the impact of land reclamation on the groundwater systems in these islands. Though a number of studies using analytical and physical methods have been conducted to explore some quantitative indicators in a homogeneous oceanic island or coastal aquifers (Lu et al., 2019; Yan et al., 2021; Zhang et al., 2021), these conceptual models are two dimensional with symmetric and may not be suitable for the tropical coral islands. For example, the thicknesses of the reclamation area on reef flat are usually small and occur only on one side of coral islands in practice, so the water divide will shift and not always be at the center of the model. Besides, the influences of the reclaimed materials and scales on the groundwater system in an island that has already achieved a steady-state have not been explored hed by previous studies. Furthermore, considering the special aquifer structure of the coral islands in the tropical oceans (e.g., dual-aquifer system, un- or poorly consolidated Holocene sediments deposited unconformably on Pleistocene limestone reef deposits) (Werner et al., 2017), the thickness or storage of the fresh groundwater lens may not follow a general solution derived from a single aquifer system.

The overall objective of this study is to explore the effects of the reclaimed materials and scales on an island that already has a steady fresh groundwater lens. To achieve the objectives, multiple methods such as sharp-interface analytical solutions, laboratory sand-tank experiments (physical simulations), and numerical simulations are used to provide solid observations and findings on the influences of land reclamation on the groundwater system in an existing oceanic island that has already formed a fresh groundwater lens. Moreover, a field-scale land reclamation case on Yongxing Island (South China Sea) has also been investigated to cross-validate the findings obtained from laboratory-scale observations. It is believed that the results obtained from this study can provide a better understanding of the evolution of fresh groundwater lens in an oceanic island after land reclamation.

2. Conceptual Model

Land reclamation on tropical coral islands is usually carried out on shallow reef flats within 5 m depth, and the fill materials are collected from the surrounding lagoon sediments or gravels from the excavation of adjacent ports. Therefore, the upper aquifer consists of two parts: (1) the original island and (2) the reclamation area (Figure 1b). The conceptual model describing the cross-section of an idealized strip island with a constant recharge rate w $[L/T]$ is shown in Figure 2. Before reclamation, the original width of the island is L_1 $[L]$. The aquifer has a uniform hydraulic conductivity, K_1 $[L/T]$ with a thickness of H_0 $[L]$. The origin of the coordinates ($x = 0, z = 0$) is set at the bottom left coastline, while the z axis is oriented parallel to the gravity vector and along the left coastline of the cross-section, and x is the horizontal distance from the shoreline $[L]$. h_1 $[L]$ is the elevation of the water table above sea level, and z_1 $[L]$ is the distance from the mean sea level to the depth of the fresh-saline water interface. The density of seawater and freshwater are ρ_s $[M/L^3]$ and ρ_f $[M/L^3]$, respectively. x_{dr_1} $[L]$ is the distance from the left shoreline to the water divide before reclamation. Here it is assumed that land reclamation occurs on the right-hand side of the island, and the coastline is extended to the sea by L_2 $[L]$ (which is noted as reclamation scale hereafter) using fill materials that have a hydraulic conductivity K_2 $[L/T]$. The thickness of the fill materials under sea level is b_0 $[L]$ (which is noted as reclamation thickness hereafter). The porosity of the original aquifer and the fill material are assigned to be the n_1 and n_2 [-]. x_{dr_2} $[L]$ is the distance from the left shoreline to the water divide after reclamation and Δx_{dr} $[L]$ is the shift of the water divide after land reclamation. V_1 $[L^3]$ and V_2 $[L^3]$ are the freshwater storage of the lens before and after land reclamation at the steady state.

3. Material and Methods

3.1. Analytical Solution

Considering the Dupuit assumption (Dupuit, 1863) and the Ghijben-Herzberg approximation (Ghijben, 1888; Herzberg, 1901), Fetter (1972) presented the analytical solutions for the position of the fresh-saline water interface and water table in the strip and circular uniform islands with steady state groundwater flow. Vacher (1988) and Dose et al. (2014) extended Fetter's (1972) solutions for fresh groundwater lens in islands of variable hydraulic conductivities. Before land reclamation (Figure 2a), the water table and depth of the fresh-saline water interface in the oceanic island for steady-state can be expressed as (Fetter, 1972):

$$h_1 = \sqrt{\frac{w}{K_1(1+\alpha)}\left[L_1 x - x^2\right]} \tag{1}$$

$$Z_1 = \alpha \cdot h_1 \tag{2}$$

where $\alpha = \frac{\rho_f}{\rho_s - \rho_f}$. Other variables are defined earlier in the section of conceptual model. The position of the water divide is $x_{dr\_1} = L_1/2$. However, the Ghijben-Herzberg principle implicitly assumes that the depth of the interface is zero at the coastline. This is likely the consequence of neglecting the freshwater outflow in the analytical solution, leading to underestimating the lens thickness near the sea boundary. So the interface depth z_{sf} $[L]$ near the coastline in a uniform aquifer can be expressed as below (Vacher, 1988):

$$z_{sf} = \sqrt{\frac{\alpha^2 q'^2}{K^2} + \frac{2\alpha q' x}{K}} \tag{3}$$

where q' is the discharge from the aquifer at the coastline per unit width $[(L^3/T)/L]$, x is the horizontal distance measured landward from the coastline $[L]$. When $x = 0$, $z_0 = \alpha q'/K$. However, the coastal area where the above equation is applicable is about 1%–5% of the total width of the island (Vacher, 1988).

The transient development of the thickness of a fresh groundwater lens can be expressed using the analytical model derived by Stuyfzand and Bruggeman (1994):

$$t = \frac{f_1 f_2}{2} \cdot \sqrt{\left[\frac{4wK_1(\rho_s - \rho_f)}{(n_1 L_1)^2 \rho_s}\right]} \cdot \ln\left[\frac{1 + \frac{z_t}{z_\infty}}{1 - \frac{z_t}{z_\infty}}\right] \tag{4}$$

where z_t $[L]$ is the depth to the fresh-saline water interface at time t $[T]$, z_∞ is the depth to the fresh-saline water interface at time ∞ $[T]$ (or steady state, which can be obtained from Equation 2). n_1 is the effective porosity. f_1 [-] is the correction factor to account for aquifer anisotropy. Here the aquifer is assumed to be homogeneous and isotropic, therefore $f_1 = 1$. f_2 [-] is a correction factor to improve the fit to the numerical model by Bakker (1981). Here $f_2 = 1$, which is the same as the setting of the previous studies (Stoeckl & Houben, 2012).

Land reclamation usually takes place on the shallow water areas around a tropical island. The analytical solutions of the water level and the position of water divide in a strip island beyond the coastline area after land reclamation are given by Jiao and Post (2019):

$$h_{1f} = \sqrt{\frac{w}{K_1(1+\alpha)}\left(2x_{dr\_2}x - x^2\right)} \left(0 \le x \le L_1\right) \tag{5}$$

$$\frac{K_2 + \alpha K_1}{2} h_{2f}^{\ 2} + b_0(K_2 - K_1)h_{2f} = wx_{dr\_2}x - \frac{w}{2}x^2 + \frac{w}{2}(L_1 + L_2)^2 - wx_{dr\_2}(L_1 + L_2) \quad (L_1 \le x \le L_1 + L_2) \tag{6}$$

The water divide is expected to shift to the right of the island. Assume the new location is x_{dr_2},

$$x_{dr\_2} = \frac{L_1}{2} + \frac{K_1(1+\alpha)\eta^2}{2wL_1} \tag{7}$$

where:

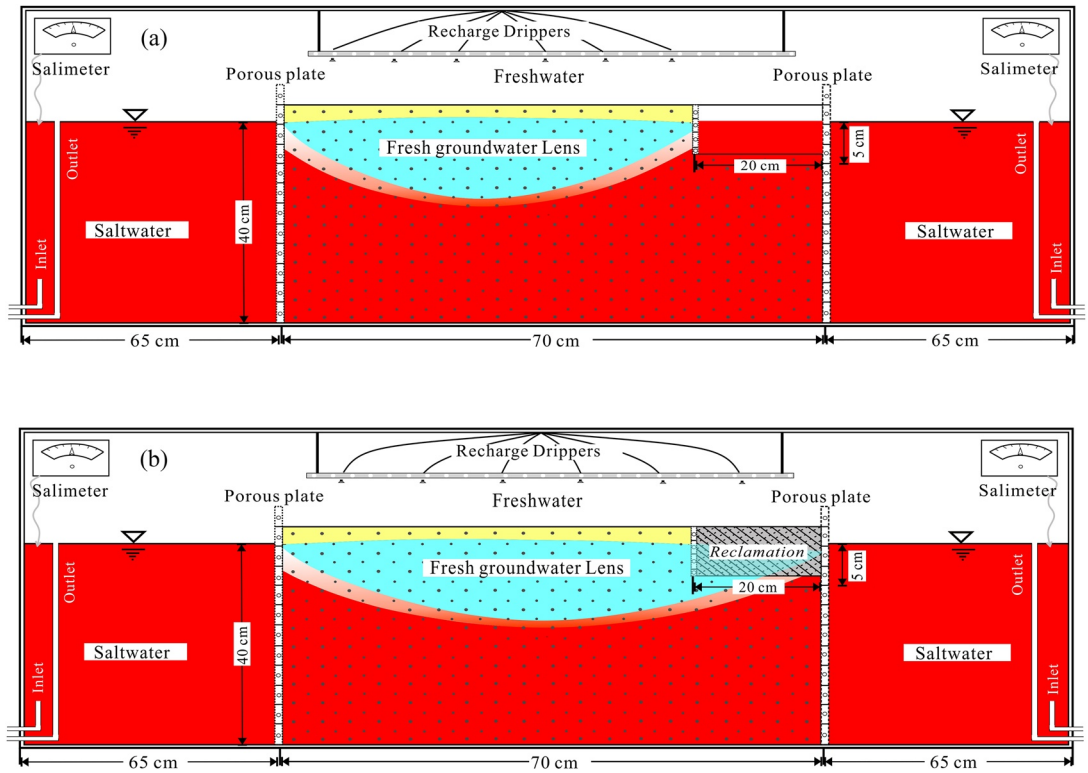

Figure 3. Schematic diagram of the sand tank setup used for the laboratory experiments to study the effect of land reclamation on an oceanic island that has already formed a fresh groundwater lens. (a) A homogeneous island before land reclamation, (b) a homogeneous island after land reclamation.

$$\eta = \frac{\sqrt{v^2 + 4\delta\left(L_1L_2 + L_1^2\right)} - v}{2\delta} \tag{8}$$

$$v = 2\frac{b_0L_1\left(K_2 - K_1\right)}{wL_2} \tag{9}$$

$$\delta = \frac{L_1K_2 + L_2K_1 + K_1\left(L_1 + L_2\right)\alpha}{wL_2} \tag{10}$$

From Equation 7, the shift of the water divide to the right after land reclamation is:

$$\Delta x_{\mathrm{dr}} = x_{\mathrm{dr\_2}} - x_{\mathrm{dr\_1}} = \frac{K_1\left(1+\alpha\right)\eta^2}{2wL_1} \tag{11}$$

The freshwater storage at the steady state before (V_1) and after (V_2) land reclamation in this study can be deduced by integrating the freshwater thickness over the whole island [L^3]:

$$V_1 = n_1\int_{x=0}^{x=L_1}\left(z_1 + h_1\right)dx \tag{12}$$

$$V_2 = n_1\int_{x=0}^{x=L_1}\left(z_{1f} + h_{1f}\right)dx + n_2\int_{x=L_1}^{x=L_1+L_2}\left(b_0 + h_{2f}\right)dx + n_1\int_{x=L_1}^{x=L_1+L_2}\left(z_{2f} - b_0\right)dx \tag{13}$$

The increase in freshwater storage ΔVs after land reclamation can be easily obtained by subtracting Equation 12 from Equation 13, $\Delta V = V_2 - V_1$.

3.2. Laboratory Experiments

The dimensions of the setup of the sand-tank laboratory experiments are 200 cm (length)×50 cm (height)× 10 cm (width) (Figure 3). The experimental setup is divided into three zones by two porous plates: saltwater reservoirs on the left and right (to simulate ocean) and porous medium chamber (to simulate oceanic

island) between them. Medium filter sand (quartz sand with a uniform diameter of 0.425 mm) is used to fill in the porous medium chamber at the center to form the unconfined aquifer in the oceanic island. The sea level and concentration are maintained constant through outlet and inlet tubes, by which saltwater will be drained when the sea level is higher than the top of the outlet (40 cm above the tank bottom). Since freshwater continuously discharging into the sea could dilute the saltwater in the saltwater reservoirs, two inlet tubes are used to supply saltwater (35 g/L) continuously to maintain the constant concentration of the fluid in the saltwater reservoirs.

Sodium chloride (NaCl) solution with a concentration of 35 g/L was prepared to represent seawater (which is referred to as saltwater hereafter). Saltwater was injected to saturate the sand from the bottom to minimize the air being entrapped in pores. Two salimeters (SmartSensor AR8212, 0.0–50.0 g/L, resolution ratio: 0.1 g/L) were used to measure the concentration of saltwater reservoirs. Densities of freshwater (ρ_f) and saltwater (ρ_s) were determined to be 1,000 and 1,025 kg/m^3, respectively. Freshwater was recharged into the island's unconfined aquifer through 6 individual freshwater drippers with a total rate of 0.1 cm/min driven by a multichannel peristaltic pump (Longerpump® BT100-1L, China), equivalent to 50 mL/min as the total flux. For visualization, the dye tracer uranine (yellow) was added to the freshwater at a concentration of 0.3 g/L. It was verified by multiple sand-tank laboratory experiments that the dyes could migrate synchronously with the saltwater in the flow tank (Dose et al., 2014; Stoeckl & Houben, 2012; Stoeckl et al., 2015). The porosity was measured at 0.45. The average hydraulic conductivity (K_1) of the medium filter sand was determined to be 2.1×10^{-3} m/s using the Kozeny-Carman empirical equation (Carman, 1937; Odong, 2008) together with the Darcy column tests. Experimental results were recorded by a digital camera (Canon EOS 90D) with a time interval of 5 min. After the fresh groundwater lens is kept under the steady state for more than 1 h (the fresh-saline water interface no longer changes), more medium filter sands are added to the top right of the island to simulate the land reclamation (20 cm (length)×5 cm (depth)). Finally, the area of the island surface is increased from 0.05 to 0.07 m^2 (Figure 3b) and the recharge rate is kept to be the same as before and this rate is also applied to the reclamation area (the total flux of freshwater is increased from 50 to 70 mL/min). The temperature of the laboratory was monitored and kept constant throughout the experiment (24°C) by the air conditioner.

3.3. Numerical Modeling

The numerical simulation used in this study was carried out using SEAWAT (Langevin, 2008), a finite difference model considering the variable-density groundwater flow and solute transport. Aquifer properties (such as hydraulic conductivity and porosity) and boundary conditions were based on the laboratory settings, but the unsaturated zone was not considered. The upper boundary of the island was represented by a specified flux boundary with a recharge rate of 0.1 cm/min and NaCl concentration of 0 g/L. The bottom of the model was set as a no-flow boundary. The left-side and right-side saltwater boundaries were set to a constant head of 40 cm, and a constant concentration of 35 g/L.

The simulation area was a homogeneous and unconfined vertical cross section of 70 × 40 cm, which is discretized by uniform grid with quadratic elements with an edge length of 0.5 cm. Considering the cell sizes and potential lengths of flow paths, the longitudinal dispersivity (α_L) and transversal dispersivity (α_T) were set to be 0.5 and 0.05 cm respectively, which were based on the parameter values used in similar fresh groundwater lens models by Stoeckl and Houben (2012), Dose et al. (2014) and Stoeckl et al. (2015). The grid spacing and dispersivity satisfied the Peclet number criterion to ensure numerical stability (Voss & Souza, 1987):

$$\mathrm{Pe} = \frac{v\Delta L}{D + a_L v} \approx \frac{\Delta L}{a_L} = 1 < 4 \tag{14}$$

where ΔL is the grid spacing, D is molecular diffusion. An initial time step of 0.001 min was adopted for all simulations, with a time step multiplier of 1.2. The maximum allowed time step size was set to 0.02 min. The total simulation time for each model was 500 min. Before the fresh groundwater lens was formed in the oceanic island, the initial concentration and hydraulic head for the model was set as 35 g/L and 40 cm respectively. After the model reaches a steady state, the results of the model before land reclamation (concentration and hydraulic head distributions) were used as the initial condition for the simulation with land reclamation. In this model, the reclamation area has the same boundary (recharge rate and concentration) settings as the model before reclamation.

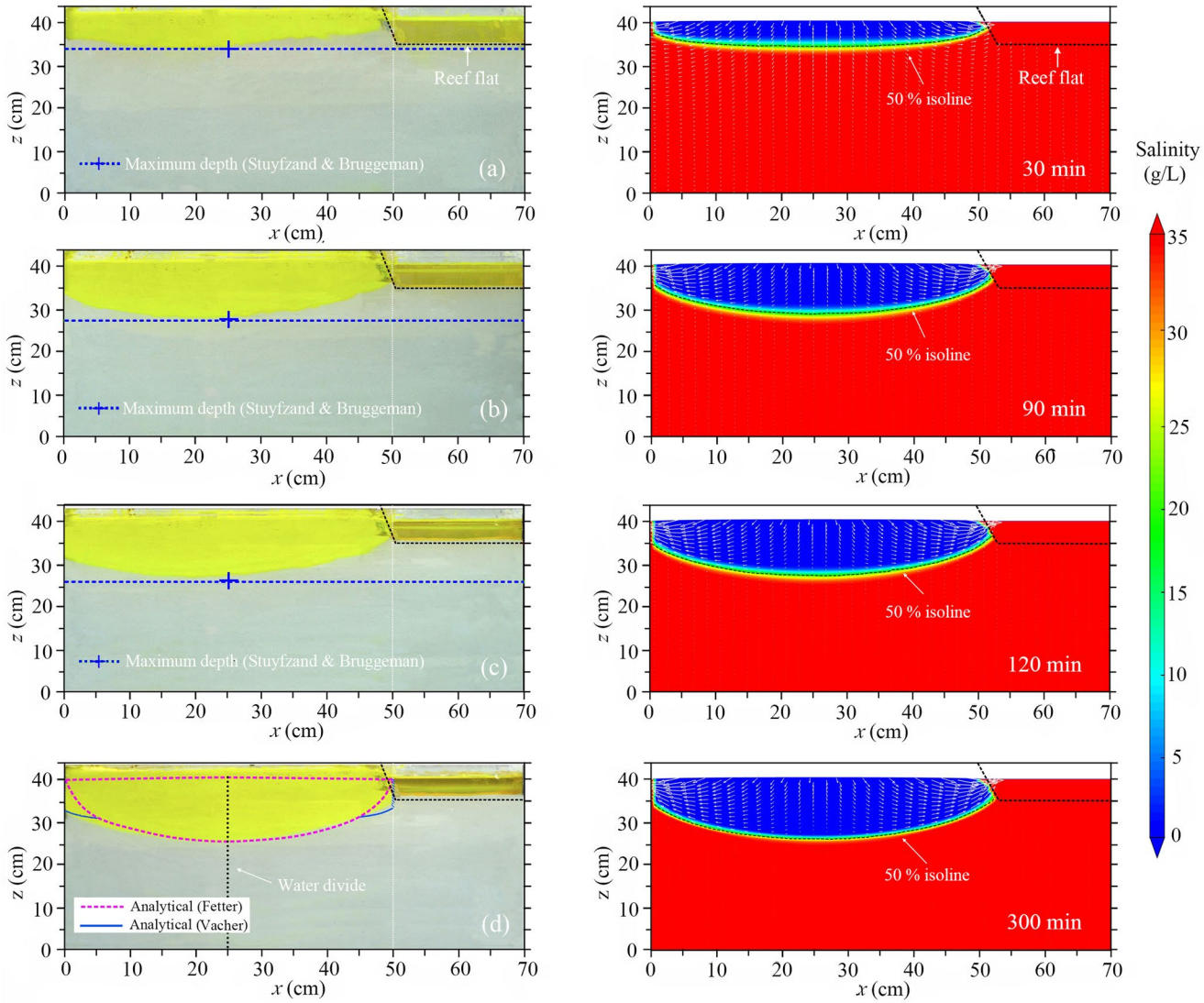

Figure 4. Comparison of sand-tank experimental (left panels), analytical (the dotted and solid lines in the left panels), and numerical results (right panels); (a, b, c, and d) represent the geometric characteristics of the fresh groundwater lens at 30, 90, 120 and 300 min. For comparison, the simulated 50% isolines of the seawater are extracted from the numerical results.

4. Results

4.1. Formation of Fresh Groundwater Lens Before Reclamation

The fresh groundwater lens at different stages in physical, analytical, and numerical models was visualized in Figure 4, which shows that a relatively sharp saline water interface is developed. The analytical solutions and numerical simulation results match well with the laboratory experiments at different times during the formation of the fresh groundwater lens, especially consistent with the 50% isoline from numerical results. For example, based on the numerical simulation, the maximum thickness of the fresh groundwater lens was 6.1, 12.5, and 13.5 cm at 30, 90, and 120 min, respectively, which was comparable to analytical solutions (5.9, 12.0, and 13.0 cm) based on the equation derived by Stuyfzand and Bruggeman (1994). At the steady state, there is only a 2% difference in the maximum thickness of the fresh groundwater lens between the numerical simulation and laboratory experiments (14 vs. 14.3 cm). The final position of the water divide was obtained as $x_{dr\_1} = 25$ cm from all three models. Overall, the numerical model reproduces well the formation process of fresh groundwater lens observed in the sand tank laboratory experiments.

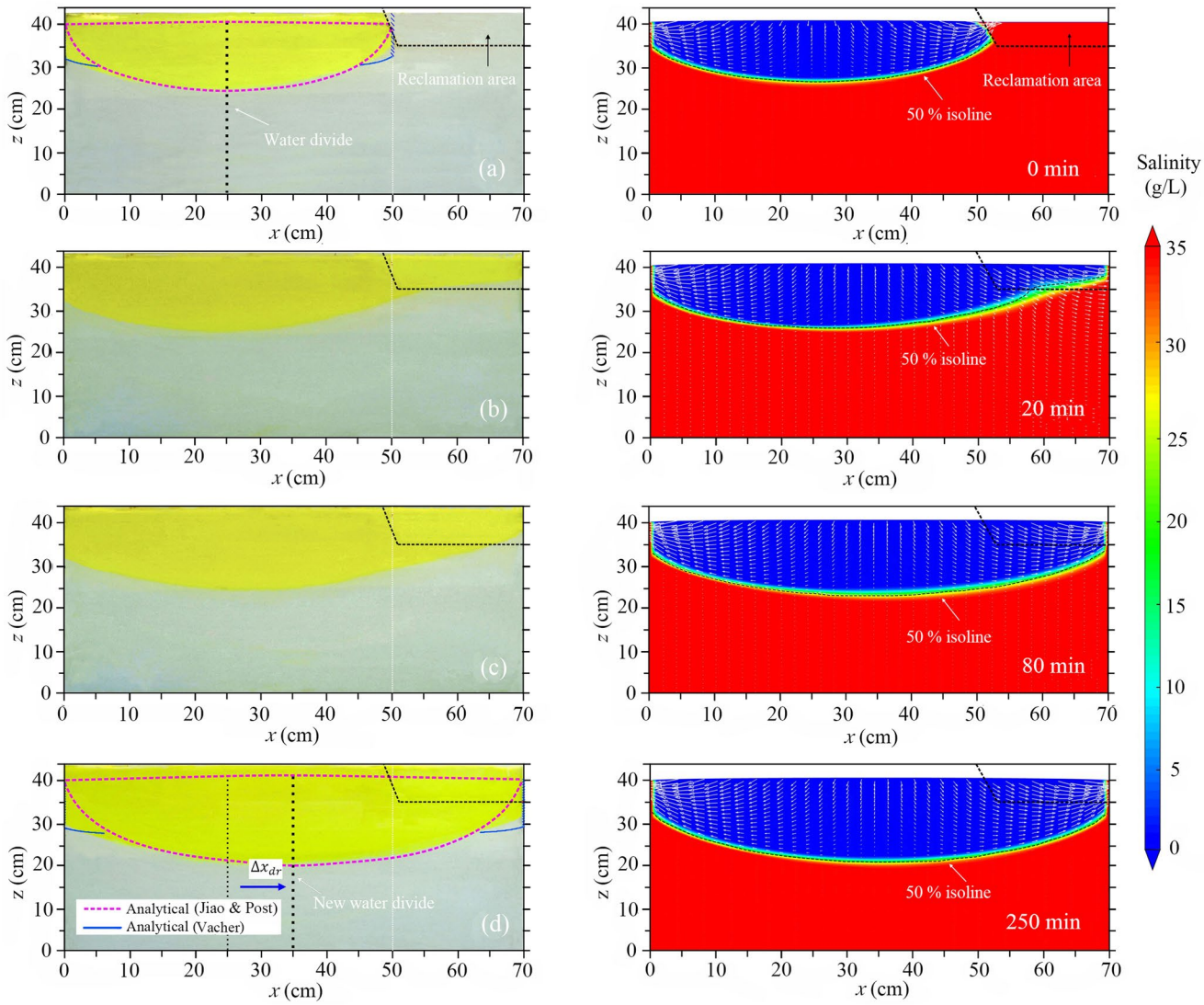

Figure 5. Comparison of sand-tank experimental (left panels), analytical (the dotted and solid lines in the left panels), and numerical results (right panels) after land reclamation; (a, b, c, and d) represent the geometric characteristics the fresh groundwater lens at 0 min (immediately after reclamation), 20, 80 and 200 min. For comparison, the simulated 50% isolines of the seawater are extracted from the numerical results.

The analytical solution differs from the sand-tank experimental and numerical results primarily in the region near the sea boundary. The depth of the fresh-saline water interface at the $x = 0$ is 7 and 8 cm based on the numerical model and sand-tank laboratory experiments but equals to 0 based on analytical solution from Fetter (1972). This is mainly because the analytical solution does not consider the freshwater outflow zone, leading to underestimating the lens thickness near the sea boundary. Therefore, a simple analytical model has been developed in this area (Equation 3), and the depth of the fresh-saline water interface at the $x = 0$ is estimated to be 8.3 cm. For fresh groundwater storage V_1 before land reclamation, all the three methods produced very similar results and the average value is about 1,117 cm^3.

4.2. Formation of Fresh Groundwater Lens After Reclamation

Land reclamation was carried out at the top right corner of the model with a width (L_2) of 20 cm and a depth (b_0) of 5 cm below the mean sea level (Figure 5). The hydraulic properties of the fill materials are the same as the original aquifer. It takes about 250 min for the model to reach a new steady state with a maximum fresh groundwater lens thickness of 19.5 cm according to the numerical results, while the maximum

Table 1
Scenario Settings With Different Fill Materials and Reclamation Scales in the Numerical Simulation

Parameters	K_2 [cm/min]	Anisotropy [-]	n_2 [-]	L_2 [cm]	b_2 [cm]
Base case	**12**	**1**	**0.45**	**20**	**5**
Case 1	**6**	1	0.45	20	5
Case 2	**18**	1	0.45	20	5
Case 3	**24**	1	0.45	20	5
Case 4	12	**3**	0.45	20	5
Case 5	12	**6**	0.45	20	5
Case 6	12	**9**	0.45	20	5
Case 7	12	1	**0.15**	20	5
Case 8	12	1	**0.25**	20	5
Case 9	12	1	**0.35**	20	5
Case 10	12	1	0.45	**5**	5
Case 11	12	1	0.45	**7.5**	5
Case 12	12	1	0.45	**10**	5
Case 13	12	1	0.45	**12.5**	5
Case 14	12	1	0.45	**15**	5
Case 15	12	1	0.45	**17.5**	5
Case 16	12	1	0.45	20	**1**
Case 17	12	1	0.45	20	**2.5**
Case 18	12	1	0.45	20	**7.5**
Case 19	12	1	0.45	20	**10**
Case 20	12	1	0.45	20	**12.5**
Case 21	12	1	0.45	20	**15**

thickness of the fresh groundwater lens is 20 cm based on the physical and analytical results. The shifts of the water divide to the right (Δx_{dr}) after land reclamation estimated from the three methods are all 10 cm. The depth of the fresh-saline water interface at $x = 0$ is 9.5 and 10 cm based on the numerical model and sand-tank experiments, and 11.7 cm from Equation 3. The average fresh groundwater storage after reclamation (V_2) is 2,069 cm^3. Although the land reclamation scale (L_2 =20 cm) only accounts for 40% of the width of the original island (L_1 =50 cm), the time for the groundwater system to reach a new steady state is more than 80% of the time needed to form the fresh groundwater lens after the island was created, and this phenomenon indicates that the response of the groundwater system to the land reclamation is slow. The observation in this study is coincidental with the findings in the previous studies (Hu & Jiao, 2014; Jiao et al., 2001; Jiao & Post, 2019). In general, all three approaches produced very similar results, highlighting the reliability of the benchmark models.

5. Discussion

To remove the scale effect, the influences of fill materials and scale of the reclamation area were explored through the dimensionless parameterization based on the results before land reclamation. These dimensionless parameters are distinguished using a star symbol (*), which are defined: $L^*_2 = L_2/L_1$, $b^*_2 = b_2/b_0$, $K^*_2 = K_2/K_1$, $n^*_2 = n_2/n_1$, $h^*_2 = h_2/H$, $z^*_2 = z_2/Z$, $x^*_{dr} = x_{dr}/x_{dr\_1}$, $h^* = h/h_1$, $z^* = z/z_1$ and $\Delta V^* = V/V_1$ (here: $L_1 = 50$ cm, $b_0 = 5$ cm, $K_1 = 12$ cm/min, $H = 0.4$ cm, $Z = 14$ cm, $x_{dr\_1} = 25$ cm, and $V_1 = 1{,}117$ cm^3,which are obtained from the results before land reclamation). Here the anisotropy is defined as the ratio of the horizontal to vertical hydraulic conductivity (K_x/K_v). Given that the numerical method has been verified by laboratory sand-tank experiments and analytical solutions, the numerical method is reliable and will be used to explore the influence of many factors on the fresh groundwater lens after land reclamation. On the other hand, tropical coral islands, usually composed of two aquifers formed by poorly consolidated Holocene sediments deposited unconformably on karstified Pleistocene limestone reef deposits (Werner et al., 2017), differ from other small uniform islands. For example, Holocene sediments usually have much lower K values than the karstified Pleistocene deposits, and the difference in K typically can be one to two orders of magnitude (Bailey et al., 2012). Therefore, a high K (120 cm/min) layer is given to the bottom aquifer (between the elevation of 0–25 cm) to compare the response of fresh groundwater lens in such specific hydrogeological structure or uniform island to the same land reclamation.

5.1. Influences of Fill Materials on Fresh Groundwater Lens After Reclamation

Previous studies indicated that the hydraulic properties of coral sand or fill materials exhibit highly spatial heterogeneity (Sheng et al., 2020; Werner et al., 2017). For example, Bailey et al. (2010) found that the sediments of the leeward oriented islands are much finer than the windward oriented islands in the Federated State of Micronesia, due to protection from wind and waves. However, when the fill materials are pumped out through a duct, the particles will be deposited in different zones under the influence of their own gravity. Therefore, 10 numerical simulations were designed to further explore the effects of fill materials on fresh groundwater lens (Base case to Case 9 in Table 1). The horizontal hydraulic conductivity, anisotropy (K_x/K_v), and porosity here were included to explore the effects of different fill materials on the distribution and growth of the fresh groundwater lens while the other parameters are kept the same as the base case.

Figure 6 illustrates the effects of fill materials with different hydraulic properties on the water table, fresh-saline water interface, and fresh groundwater storage. Compared with other hydraulic parameters, hydraulic

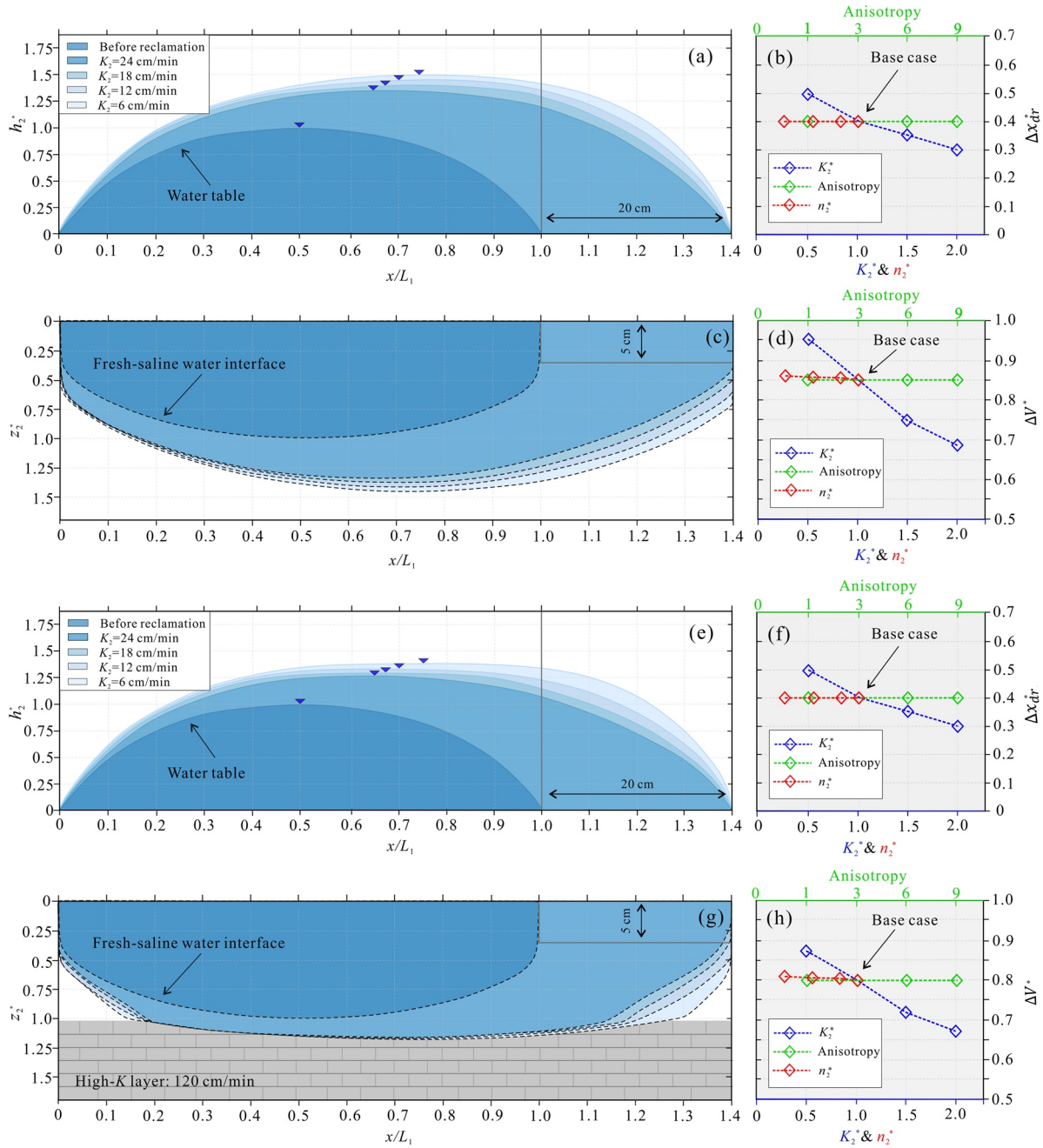

Figure 6. The change of the geometry of the fresh groundwater lens with different fill materials in the uniform (a–d) or dual-aquifer (e–h) system: (a and e) water table, (c and g) fresh-saline water interface, and variation of dimensionless water divide (b and f) and freshwater storage (d and h) with fill materials of different hydraulic conductivities, anisotropy, and porosity (note: the reclamation area is located in the top right corner).

conductivity has the greatest influence on the fresh groundwater lens. Specifically, with the decrease of the hydraulic conductivity of the fill materials, the thickness and storage of the fresh groundwater lens gradually increase compared to the base case. For example, when the hydraulic conductivity of the fill materials was the same as the original aquifer ($K^*_2 = 1$), the fresh groundwater lens was symmetric at the steady state. The shift ratio of the water divide Δx^*_{dr} is 0.4. The increased ratios of the water table and the depth of the fresh-saline water interface at the water divide are 0.37 and 0.39 respectively compared to the results before reclamation. However, when the hydraulic conductivity of the fill materials decreased by 50% relative to the original aquifer ($K^*_2 = 0.5$), the shift ratio of the water divide Δx^*_{dr} is 0.5 and the increased ratios of the

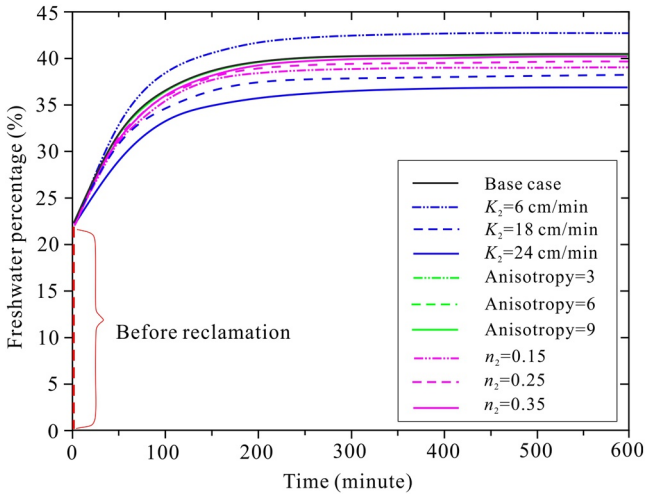

Figure 7. Formation process of the fresh groundwater lens under different fill materials. The freshwater percentage is the ratio of the freshwater volume to the total volume of the water in the numerical model.

water table and the depth of the fresh-saline water interface at the water divide are 0.45 and 0.46 respectively.

In general, the fresh groundwater lens is no longer as a symmetrical "lens" when the hydraulic conductivity is different from the original aquifer. However, the fresh groundwater lens was not sensitive to the anisotropy or vertical hydraulic conductivity, because the aquifer is dominated by the horizontal flow. Besides, a constant boundary is assumed here and the effects of the tidal fluctuation are overlooked which influence the vertical flow and the release or compression of water (Underwood et al., 1992). The observed phenomenon is in accordance with the finding in the previous study by Yao et al. (2019). It is obvious that a refraction occurs at the unconformity interface and a higher K will truncate the lens and cause the lens to become thinner (Figure 6g) compared to the case of a single-layer system. However, it has a relatively limited effect on the water table: the water table at the center area of the island will drop slightly (Figure 6e), but the position of the water divide will not change much (Figure 6f).

Fresh groundwater lens is stored in the pores of the aquifer. Therefore, the porosity will affect the maximum storage of the fresh groundwater lens and the flow rate under the same hydraulic gradient. A large porosity leads to more water in storage, but this also means that more salt water will be initially stored in the fill materials, and thus more freshwater recharge is needed to flush out the salt water in the pores (Yao et al., 2019). However, the geometry of the fresh groundwater lens and the position of the water divide in this study seem not sensitive to the porosity of the fill materials (Figure 6), even the formation time of the fresh groundwater lens to reach the steady state remains consistent after reclamation (Figure 7). This finding is very different from Yao et al. (2019). This is probably because the proportion of the volume of the fill materials to total aquifer volume is very small (only 3.57%) and the fill materials mainly occupy the upper right of the model. Therefore, the effect of porosity on the fresh groundwater lens is limited.

Figure 8 shows the impact of fill materials on the groundwater flow system and the seaward groundwater discharge in the island after reclamation. In comparison to the original island, the seaward groundwater discharge will be reduced because the land reclamation increases the subsurface flow path length, causing an increase in the water level in the aquifer. When the fill material is less permeable than the original aquifer, the fill materials will force some of the fresh groundwater to flow to the sea via the original aquifer below the reclamation site (i.e., Figure 8a, see also Movie S2, Supporting Information), which is basically the same as the experimental results of the fringing reef case studied by Houben et al. (2018). However, if the fill material is much more permeable than the original aquifer, the seaward groundwater discharge will occur mainly through the reclamation site directly (i.e., Figure 8b, see also Movie S3, Supporting Information).

5.2. Influences of Reclamation Scales on Fresh Groundwater Lens

The effects of reclamation scales (L_2) on fresh groundwater lens are shown in Figure 9 for the considered scenarios (*Cases* 10–15). Assume that the parameters of the fill materials are the same as Case 1 in Table 1. The water table, thickness, and freshwater storage of the fresh groundwater lens are all increased with the reclamation scale both in the single and dual aquifer systems. Especially in the single aquifer, the shift ratio of the water divide Δx^*_{dr} and the increased ratio of the freshwater storage ΔV^* present a linear relationship with the reclamation scale (Figures 9a and 9b). For example, when the reclamation scale (L^*) is 0.3 in the single-layer aquifer, the shift ratio of the water divide Δx^*_{dr} is 0.38. The increased ratio of the water table Δh^* and the depth of the fresh-saline water interface Δz^* is 0.35 and 0.36 at the water divide. However, when the reclamation scale (L^*) is 0.4 in the single-layer aquifer, the shift ratio of the water divide Δx^*_{dr} is 0.5 and the increased ratio of the water table Δh^* and the thickness of the saline interface Δz^* is 0.45 and 0.43.

In the dual-aquifer system in most tropical coral islands, when the fresh groundwater lens is thin and not beyond the unconformity interface, the lens development is similar to that in the single-layer or homogeneous

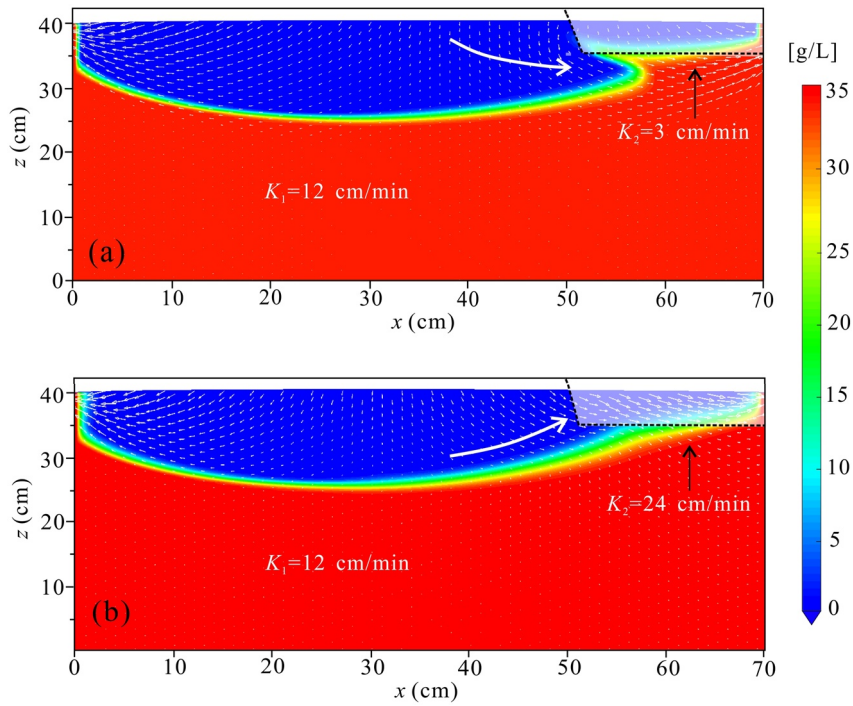

Figure 8. The impact on groundwater flow system and the seaward groundwater discharge in island after land reclamation. (a) K_2 of the fill material is 3 cm/min; (b) K_2 of the fill material is 24 cm/min.

island (Figures 9a and 9c). However, with the increase of reclamation scale, the thickness of the fresh groundwater lens continues to increase, and the fresh groundwater lens will eventually penetrate into the more permeable base layer. Therefore, the lens will be truncated by the unconformity interface (Supporting Information, Movie S1). The water table at the center area of the island will drop slightly but the position of the water divide does not change much compared to the single-aquifer system. For example, when the reclamation scale (L^*) changes from 0.3 to 0.4, the increased ratio of the water table Δh^* changes from 0.31 to 0.36, but the increase ratio of the depth of the fresh-saline water interface Δz^* remains to be 0.29. Therefore, it seems that there is a critical reclamation scale beyond which the thickness of the fresh groundwater lens in the tropical coral island with such a dual-aquifer system will not increase anymore. However, the freshwater storage will always continue to increase with the reclamation scale.

5.3. Influences of Reclamation Thicknesses on Fresh Groundwater Lens

The effects of reclamation thicknesses on fresh groundwater lens are shown in Figure 10 for various scenarios (*Cases* 16–21). The parameters of the fill materials are the same as the Case 1 in Table 1. As the reclamation thickness (b_0) increases from 1 to 15 cm (b^*_2 from 0.2 to 3), both water table and depth of the fresh-saline water interface of fresh groundwater lens increase. However, the increase of the lens becomes slower or even constant when the thickness of reclamation increases to a certain value (Figures 10d and 10h). For example, when the reclamation thickness increased to 12.5 cm or 15 cm (b^*_2 is 2.5 or 3), the shift of the water divide and changes of the freshwater storage are almost negligible in all cases (Figures 10b, 10d, 10f, and 10h). Lu et al. (2019) studied the performance of low-permeability and fully penetrating barriers along the shoreline of islands in terms of the increase in the fresh groundwater storage. However, this section indicates that partially penetrating barriers of sufficient depth may have the same effect to increase the fresh groundwater storage to the fully penetrating barriers.

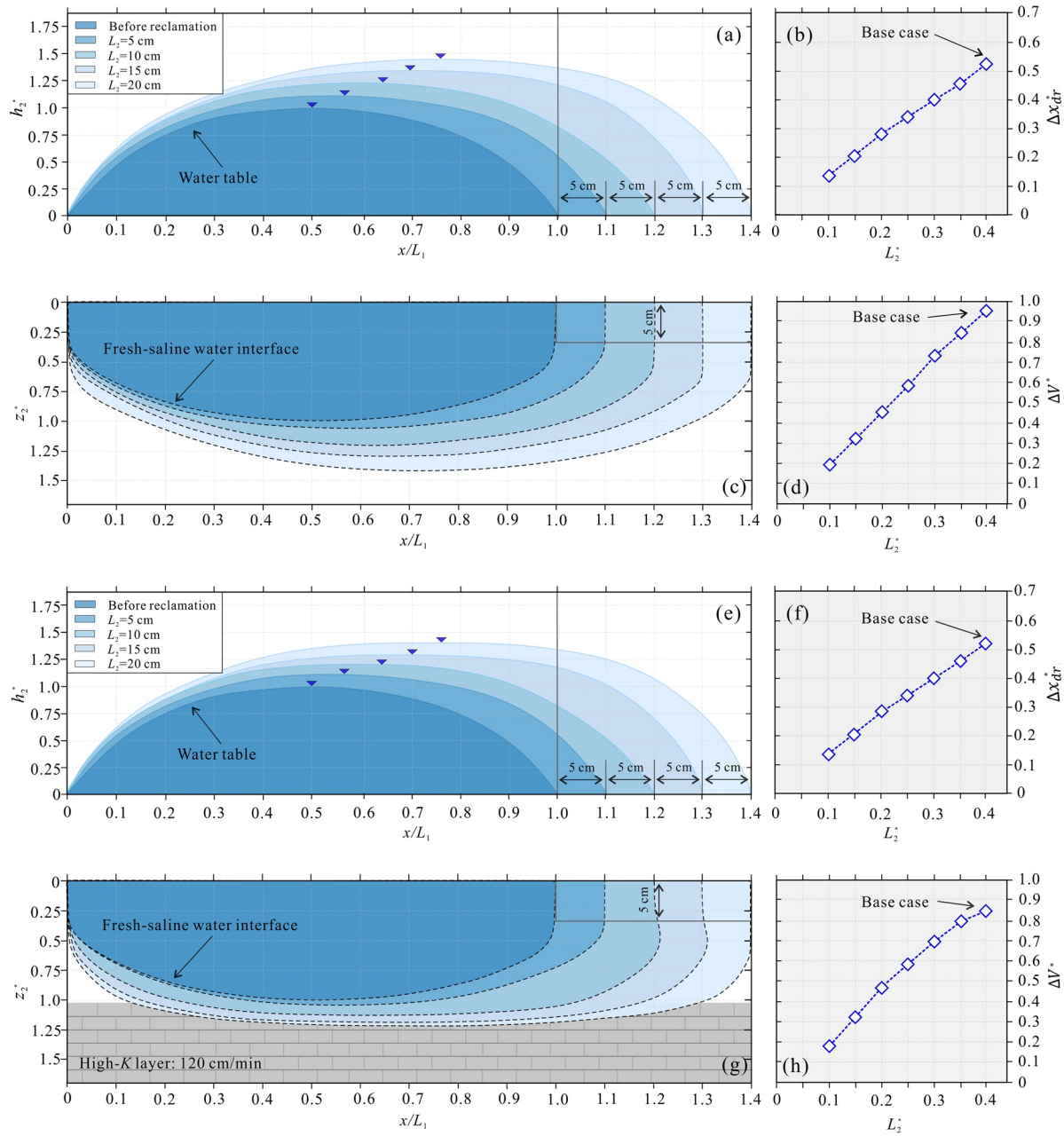

Figure 9. The change of the geometry of the fresh groundwater lens with different reclamation scales in the uniform (a–d) or dual-aquifer (e–h) system: (a and e) water table, (c and g) fresh-saline water interface, and variation of dimensionless water divide (b and f) and freshwater storage (d and h) with different reclamation scales (note: the reclamation area is located in the top right corner).

5.4. Case Study in Yongxing Island, South China Sea

To further support the observations and findings from the laboratory and theoretical discussion above, numerical simulation was conducted in Yongxing Island, which is a typical coral island with land reclamation in the Xisha Islands, South China Sea (Figure 1). The measured thickness of the fresh groundwater lens is about 14–15 m before reclamation (Zhou et al., 2010). The average annual rainfall is about 1,509 mm and the contact between the Holocene and underlying Pleistocene sediments occurs at 22 m below ground surface (shown as Figure 1b above). Other details on meteorology and hydrogeology of this field site are discussed in previous studies (Sheng et al., 2017; Zhou et al., 2009). The area of the original Yongxing Island was

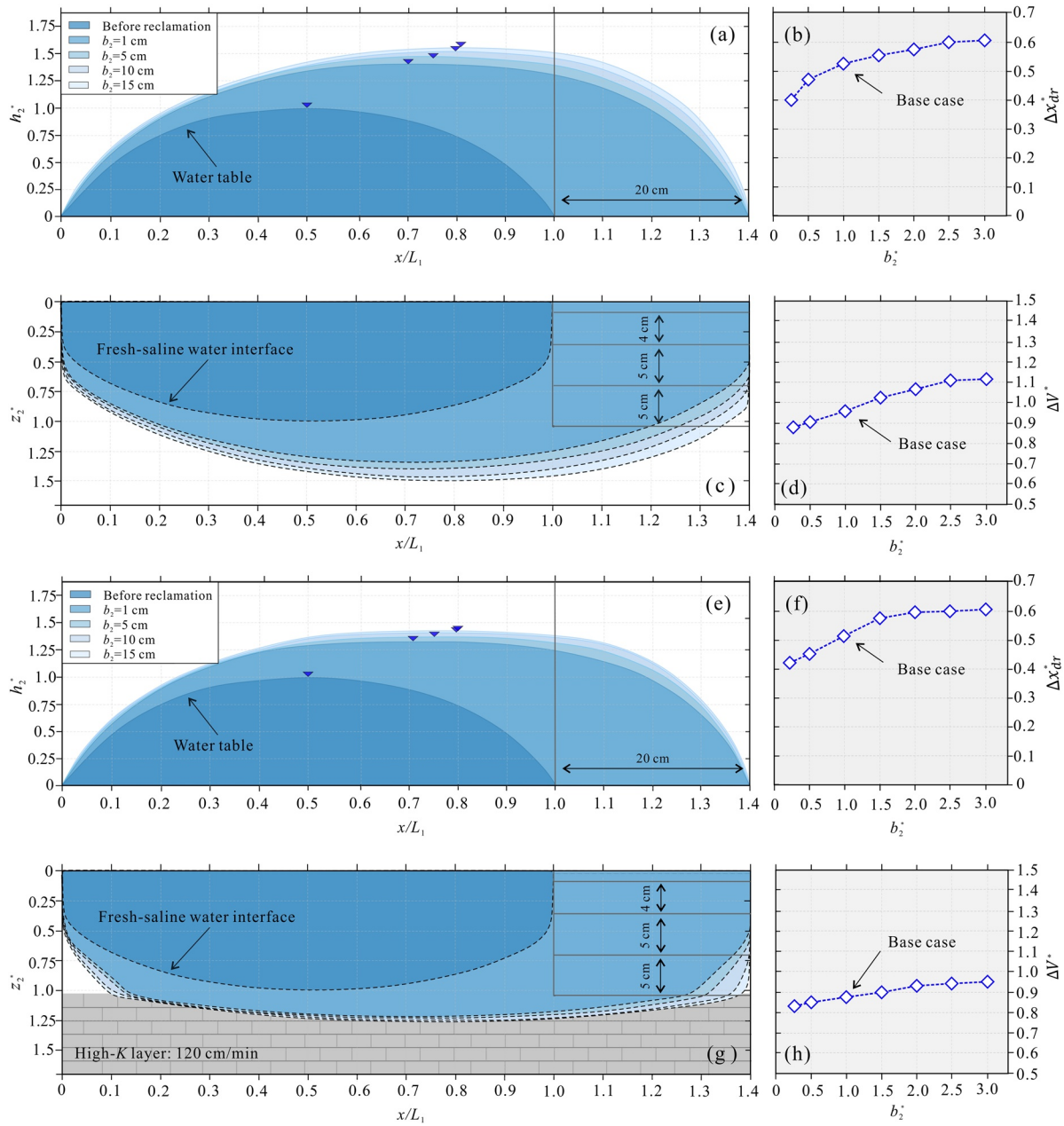

Figure 10. The change of the geometry of the fresh groundwater lens with different reclamation thicknesses in the uniform (a–d) or dual-aquifer (e–h) system: (a and e) water table, (c and g) fresh-saline water interface, and variation of dimensionless water divide (b and f) and freshwater storage (d and h) with different reclamation scales (note: the reclamation area is located in the top right corner).

2.13 km^2 and increased to 3.2 km^2 after land reclamation on the north of the island (Figures 11a and 11c). At present, the third phase of the land reclamation project is in progress. The model parameters of the original island and fill materials are based on a previous study (Sheng et al., 2017), which is summarized in Table 2.

The field-scale numerical model was run for about 40 years to obtain a steady state condition of the groundwater system in the Yongxing Island before land reclamation. The maximum water table and the thickness below sea level are 0.41 and 14 m respectively at the steady state (Figures 11a and 12a), and the water divide is located roughly at the center of the island. Afterward, the land reclamation was carried out at the north of the island (Figure 11c). Figure 11d presents the water table distributions after land reclamation. It is obvious that land reclamation not only increases the water table but also moves the water divide toward the

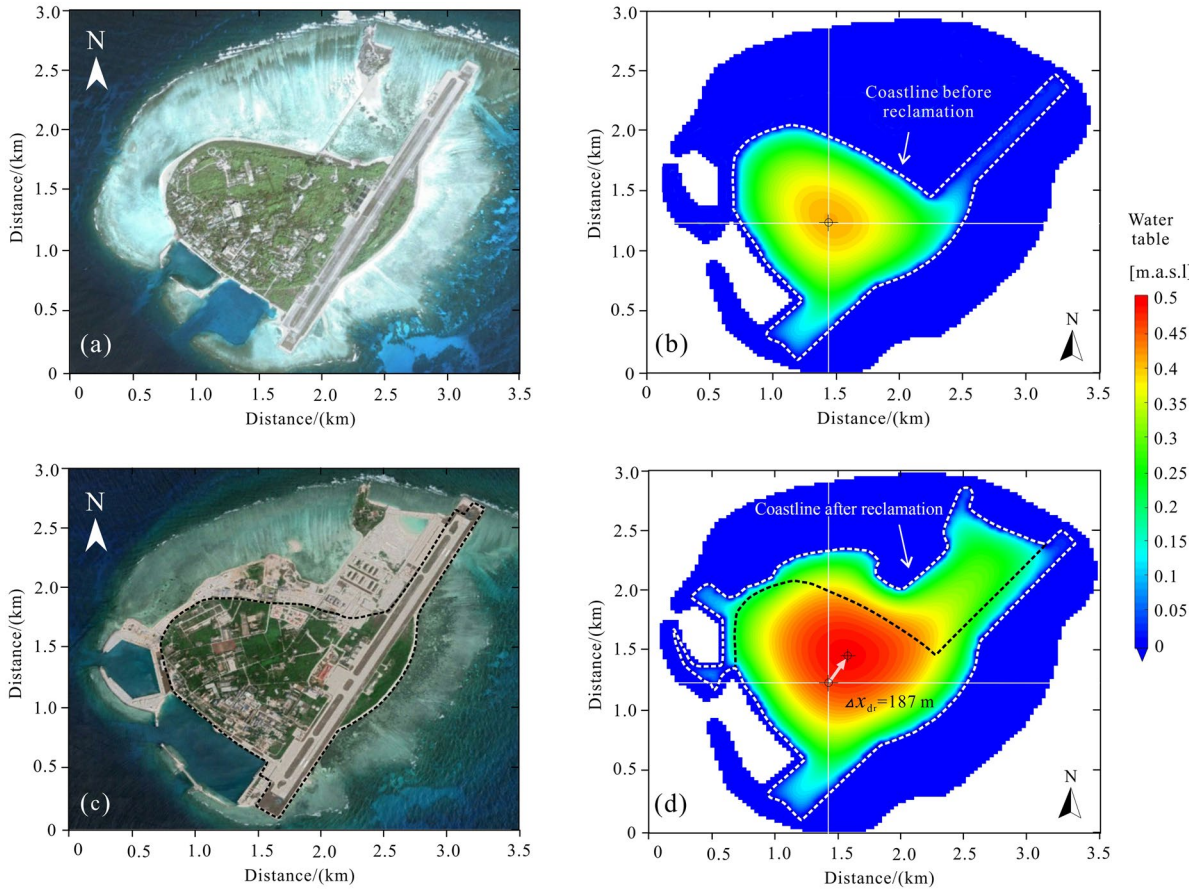

Figure 11. The change of the area and simulated water table of Yongxing Island before (a), (b) and after(c), (b) the land reclamation.

reclamation area (northeast of the island), which is consistent with the results obtained in the laboratory investigations. For example, in the direction of the movement of the water divide, the original width of the island L_1 is 1,238 m, and the reclamation scale L_2 is 248 m, therefore $L^*_2 = 0.2$. If x_{dr_1} here is the half of the total original width ($x_{dr\_1} = 619$ m), and the shift of the water divide (Δx_{dr}) in this direction is 187 m, so the Δx^*_{dr} is 0.3. Comparing to the result in Figure 9b, where the L_2* is 0.2, the Δx^*_{dr} is 0.29. This shows that the 2D model in the earlier discussion may produce reasonable results for Yongxing Island if this island is dimensionally reduced to a 2D problem.

The numerical model is run to simulate the formation of the freshwater lens in the island and the results show that it takes 25 years for the aquifer to approach a new steady state, or the formation process of the fresh groundwater lens in the island lasts 25 years after land reclamation (Figures 12b–12f). Before land reclamation, the maximum depth (14 m) of the fresh groundwater lens does not reach the interface between the Holocene sediments and the karstified Pleistocene deposits. Therefore, the aquifer before land

Table 2
Main Model Parameters in the Three-Dimensional Field-Scale Numerical Simulation

Parameters	D [m]	n [-]	b [m]	K_H [m/d]	K_P [m/d]	K_R [m/d]	α_L [m]	α_T [m]	α_v [m]	S_y [-]	S_s [-]	w [mm/y]
Value	22	0.45	6	75	500	5	5	0.5	0.05	0.14	10^{-5}	679

Note. The subscripts of H, P and R of the parameters refer to the Holocene, Pleistocene and reclamation layers, respectively, which are shown in Figure 1b, D and b are the thickness of the Holocene layer and the reclamation area under the ground surface respectively; S_y is specific yield; S_s is specific storage; the meanings of the other symbols are the same as described above.

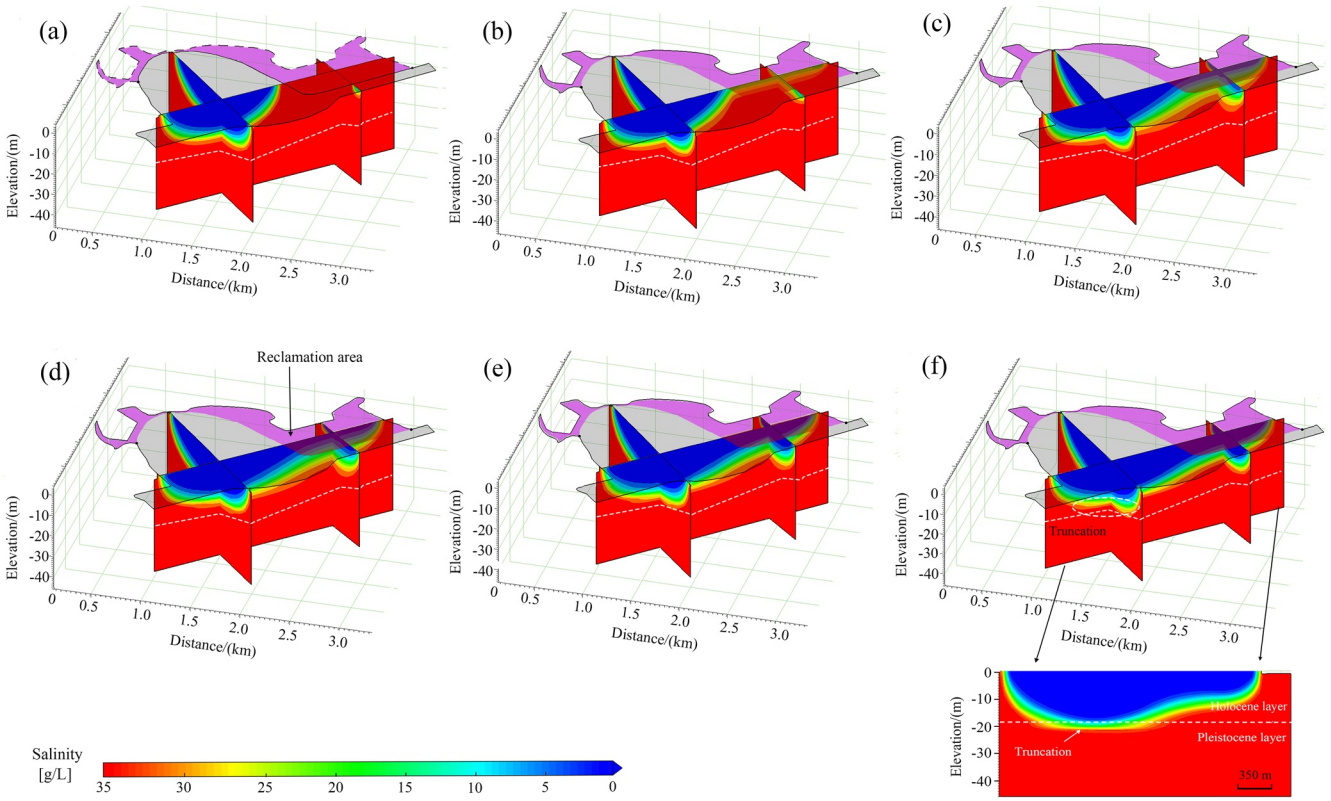

Figure 12. Formation process of the fresh groundwater lens in the Yongxing Island after the land reclamation. (a) is the steady state of the fresh groundwater lens before reclamation; (b), (c), (d), (e) and (f) are the state of the fresh groundwater lens in 1, 5, 10, 15 and 25 years after land reclamation.

reclamation can be regarded as a single layer system with uniform hydraulic properties. After land reclamation, the maximum thickness of the fresh groundwater lens below sea level increases to 17.5 m, and the fresh groundwater storage increases from 1.57×10^7 m^3 to 3.28×10^7 m^3. The field-scale study is a three-dimensional problem, therefore L_2/L_1 should be replaced by its analogue of S_2/S_1. S_2 is the area of the land reclamation and estimated to be 1.07 km^2; S_1 is the original area before reclamation and measured to be 2.13 km^2. Although the area of the island only increased by 50% ($S_2/S1 = 0.5$), the increase of the freshwater storage ΔV is nearly the same as the total freshwater storage before reclamation ($\Delta V/V_1 = 1.1$). This is similar to the result obtained from the laboratory scale investigations. When the $L_2/L_1 = 0.5$, the $\Delta V/V_1 = 1.2$ (obtained from the linear interpolation from Figure 9d).

The unconformity interface plays an important role to truncate the thickness of the transition zone (Figure 12f). It is expected that with the increase of reclamation area, the thickness of the fresh groundwater lens in Yongxing Island will continue to expand, but the depth of the lens will be constrained by the unconformity interface between the Holocene sediments and the karstified Pleistocene deposits. The results in this study indicate that the land reclamation not only provides valuable space for urban development, but also increases the potential storage of the fresh groundwater.

6. Conclusions

Land reclamation is common practice in many oceanic islands in the South China Sea and the Indian Ocean and represents a main human interference that considerably alters the natural groundwater flow system. However, so far there have been very limited studies to address the impact of land reclamation on groundwater systems in an oceanic island that has already formed a fresh groundwater lens. In this study, the analytical solutions, laboratory sand-tank experiments, and numerical models were combined to comprehensively investigate the variation of fresh groundwater storage, water table, and water divide in oceanic islands after land reclamation.

Land reclamation will increase the water table and the freshwater storage of the groundwater lens and move the water divide toward the reclamation area, but the response is in decades. The fill materials with lower horizontal hydraulic conductivity will lead to a higher water table and more fresh groundwater storage since low-permeability filling material along the shoreline retards the discharge of groundwater to the sea. However, the porosity and anisotropy of the fill materials are found to have limited influence. The fresh groundwater storage and water table of the fresh groundwater lens both increase with the reclamation scale. But the influence of the thickness of the fill materials on the fresh groundwater lens is less significant and even negligible when the thickness exceeds a certain value. For most tropical dual-aquifer islands, when the thickness of the fresh groundwater lens exceeds the depth of the unconformity interface between the Holocene sediments and the karstified Pleistocene deposits, the fresh groundwater lens will be truncated, and the lens will be thinner than the case of the single-aquifer islands. The approaches outlined in this study provide a methodology for the investigation of the impact of the land reclamation in such oceanic islands. Besides, the findings in this study are also instructive for SIDS to use the land reclamation not only for urban development but also for additional freshwater to enhance the water resource sustainability under the climate change and sea-level rise.

Data Availability Statement

The supporting data are available online (http://www.hydroshare.org/resource/1da76dc19f9c4b39adb98ccec04e657b).

Acknowledgments
This research was supported by the Strategic Priority Research Program of the Chinese Academy of Sciences (XDA13010303), Key Special Project for Introduced Talents Team of Southern Marine Science and Engineering Guangdong Laboratory (Guangzhou) (GML2019ZD0104) and the NSFC-Guangdong Joint Fund (U20A20100). The authors would also like to thank the editors and the anonymous reviewers for their constructive and valuable comments, which significantly improved the manuscript quality.

References

Bailey, R. T., & Jenson, J. W. (2014). Effects of marine over wash for atoll aquifers: Environmental and human factors. *Groundwater*, *52*(5), 694–704. https://doi.org/10.1111/gwat.12117

Bailey, R. T., Jenson, J. W., & Olsen, A. E. (2010). Estimating the ground water resources of atoll islands. *Water*, *2*(1), 1–27. https://doi.org/10.3390/w2010001

Bailey, R. T., Jenson, J. W., & Taboroši, D. (2012). Estimating the freshwater-lens thickness of atoll islands in the Federated States of Micronesia. *Hydrogeology Journal*, *21*(2), 441–457. https://doi.org/10.1007/s10040-012-0923-6

Bakker, T. W. M. (1981). *Nederlands kustduinen: Geohydrologie*. Pudoc Wageningen: Ph. D. Thesis.

Carman, P. C. (1937). Fluid flow through granular beds. *Transactions of the Institution of Chemical Engineers*, *15*, 150–166.

Chui, T. F. M., & Terry, J. P. (2012). Modeling freshwater lens damage and recovery on atolls after storm-wave washover. *Groundwater*, *50*(3), 412–420. https://doi.org/10.1111/j.1745-6584.2011.00860.x

Chui, T. F. M., & Terry, J. P. (2013). Influence of sea-level rise on freshwater lenses of different atoll island sizes and lens resilience to storm-induced salinization. *Journal of Hydrology*, *502*, 18–26. https://doi.org/10.1016/j.jhydrol.2013.08.013

Cozzolino, D., Greggio, N., Antonellini, M., & Giambastiani, B. M. S. (2017). Natural and anthropogenic factors affecting freshwater lenses in coastal dunes of the Adriatic coast. *Journal of Hydrology*, *551*, 804–818. https://doi.org/10.1016/j.jhydrol.2017.04.039

Dose, E. J., Stoeckl, L., Houben, G., Vacher, H. L., Vassolo, S., Dietrich, J., & Himmelsbach, T. (2014). Experiments and modeling of freshwater lenses in layered aquifers: Steady state interface geometry. *Journal of Hydrology*, *509*, 621–630. https://doi.org/10.1016/j.jhydrol.2013.10.010

Dupuit, J. (1863). *Étude théorique et pratique sur le mouvement des eaux dans les canaux découverts et à travers les terrains perméables [A practical and theoretical study on the flow of water in channels discovered while traversing permeable terrain]* (2nd ed.). Paris: Dunod.

Falkland, A. C. (1992). Small tropical islands: Water Resources of Paradises Lost. Waterrelated Issues and Problems of the Humid Tropics and Other Warm Humid Regions. IHP Humid Tropics Programme Series No, 2, 51.

Falkland, A. C. (1994). Management of freshwater lenses on small coral islands. In *Water Down Under 94 congress*. Australian: Adelaide, 417–422. Retrieved from http://refhub.elsevier.com/S0022-1694(17)30126-9/h0320

Fetter, C. W. (1972). Position of the saline water interface beneath oceanic islands. *Water Resources Research*, *8*(5), 1307–1315. https://doi.org/10.1029/WR008i005p01307

Ghijben, W. B. (1888). *Nota in verband me devoorgenomen putboring nabij Amserdam [Notes on the probable results of the proposed well drilling near Amsterdam]*. Amsterdam: Tijdschrift van Let Koninklijk Inst Van Ing.

Gingerich, S. B., Voss, C. I., & Johnson, A. G. (2017). Seawater-flooding events and impact on freshwater lenses of low-lying islands: Controlling factors, basic management and mitigation. *Journal of Hydrology*, *551*, 676–688. https://doi.org/10.1016/j.jhydrol.2017.03.001

Guimond, J. A., & Michael, H. A. (2021). Effects of marsh migration on flooding, saltwater intrusion, and crop yield in coastal agricultural land subject to storm surge inundation. *Water Resources Research*, *2021*, 57. https://doi.org/10.1029/2020wr028326

Gulley, J. D., Mayer, A. S., Martin, J. B., & Bedekar, V. (2016). Sea level rise and inundation of island interiors: Assessing impacts of lake formation and evaporation on water resources in arid climates. *Geophysical Research Letters*, *43*, 9712–9719. https://doi.org/10.1002/2016gl070667

Guo, H., & Jiao, J. J. (2007). Impact of Coastal Land Reclamation on Ground Water Level and the Sea Water Interface. *Groundwater*, *45*(3), 362–367. https://doi.org/10.1111/j.1745-6584.2006.00290.x

Herzberg, A. (1901). Die Wasserversorgung einer Nordseebaden [Water supply of a few hydrothermal spas in the North Sea]. *Journal of Gasbeleucht Wasserversorg*, *44*, 815-819.

Holding, S., & Allen, D. M. (2015). From days to decades: Numerical modelling of freshwater lens response to climate change stressors on small low-lying islands. *Hydrology and Earth System Sciences*, *19*(2), 933–949. https://doi.org/10.5194/hess-19-933-2015

Houben, G. J., Stoeckl, L., Mariner, K. E., & Choudhury, A. S. (2018). The influence of heterogeneity on coastal groundwater flow - Physical and numerical modeling of fringing reefs, dykes and structured conductivity fields. *Advances in Water Resources*, *113*, 155–166. https://doi.org/10.1016/j.advwatres.2017.11.024

Hu, L., & Jiao, J. J. (2014). Analytical studies on transient groundwater flow induced by land reclamation using different fill materials. *Hydrological Processes*, *28*(4), 1931–1938. https://doi.org/10.1002/hyp.9710

Hu, L., Jiao, J. J., & Guo, H. (2008). Analytical studies on transient groundwater flow induced by land reclamation. *Water Resources Research*, *44*, W11427. https://doi.org/10.1029/2008wr006926

Jiao, J., & Post, V. (2019). *Coastal hydrogeology*. New York: Cambridge University Press. https://doi.org/10.1017/9781139344142

Jiao, J. J., Nandy, S., & Li, H. (2001). Analytical studies on the impact of land reclamation on ground water flow. *Groundwater*, *39*(6), 912–920. https://doi.org/10.1111/j.1745-6584.2001.tb02479.x

Langevin, C. D. (2008). Modeling axisymmetric flow and transport. *Groundwater*, *46*(4), 579–590. https://doi.org/10.1111/j.1745-6584.2008.00445.x

Lu, C., Cao, H., Ma, J., Shi, W., Rathore, S. S., Wu, J., & Luo, J. (2019). A proof-of-concept study of using a less permeable slice along the shoreline to increase fresh groundwater storage of oceanic islands: Analytical and experimental validation. *Water Resources Research*, *55*, 6450–6463. https://doi.org/10.1029/2018WR024529

Memari, S. S., Bedekar, V. S., & Clement, T. P. (2020). Laboratory and Numerical Investigation of Saltwater Intrusion Processes in a Circular Island Aquifer. *Water Resources Research*, *56*. https://doi.org/10.1029/2019wr025325

Odong, J. (2008). Evaluation of empirical formulae for determination of hydraulic conductivity based on grain-size analysis. *The Journal of American Science*, *4*(1), 54–60.

Post, V. E. A., Bosserelle, A. L., Galvis, S. C., Sinclair, P. J., & Werner, A. D. (2018). On the resilience of small-island freshwater lenses: Evidence of the long-term impacts of groundwater abstraction on Bonriki Island, Kiribati. *Journal of Hydrology*, *564*, 133–148. https://doi.org/10.1016/j.jhydrol.2018.06.015

Röper, T., Greskowiak, J., Freund, H., & Massmann, G. (2013). Freshwater lens formation below juvenile dunes on a barrier island (Spiekeroog, Northwest Germany), Estuarine. *Coastal and Shelf Science*, *121–122*, 40–50. https://doi.org/10.1016/j.ecss.2013.02.004

Schneider, J. C., & Kruse, S. E. (2003). A comparison of controls on freshwater lens morphology of small carbonate and siliciclastic islands: Examples from barrier islands in Florida, USA. *Journal of Hydrology*, *284*, 253–269. https://doi.org/10.1016/j.jhydrol.2003.08.002

Sheng, C., Han, D., Xu, H., Li, F., Zhang, Y., & Shen, Y. (2020). Evaluating dynamic mechanisms and formation process of freshwater lenses on reclaimed atoll islands in the South China Sea. *Journal of Hydrology*, *584*, 124641. https://doi.org/10.1016/j.jhydrol.2020.124641

Sheng, C., Xu, H., & Zhang, W. (2017). Numerical simulation of the effect of geomorphologic changes on freshwater lens in the Yongxing Island. *Hydrogeology & Engneering Geology*, *45*(6), 7–14.

Stoeckl, L., & Houben, G. (2012). Flow dynamics and age stratification of freshwater lenses: Experiments and modeling. *Journal of Hydrology*, *458–459*, 9–15. https://doi.org/10.1016/j.jhydrol.2012.05.070

Stoeckl, L., Houben, G. J., & Dose, E. J. (2015). Experiments and modeling of flow processes in freshwater lenses in layered island aquifers: Analysis of age stratification, travel times and interface propagation. *Journal of Hydrology*, *529*, 159–168. https://doi.org/10.1016/j.jhydrol.2015.07.019

Storlazzi, C. D., Gingerich, S. B., van Dongeren, A., Cheriton, O. M., Swarzenski, P. W., Quataert, E., et al. (2018). Most atolls will be uninhabitable by the mid-21st century because of sea-level rise exacerbating wave-driven flooding. *Science Advances*, *4*(4). https://doi.org/10.1126/sciadv.aap9741

Stuyfzand, P. J., & Bruggeman, G. A. (1994). Analytical approximations for fresh water lenses in coastal dunes. In *Proceedings of 13th salt water intrusion Meeting* (pp. 15–33). Cagliari, Italy. Retrieved from http://www.swim-site.nl/pdf/swim13/20120516104138443.pdf

Tang, Y., Yan, M., Wang, X., Lu, C., & Luo, J. (2021). Analytical solution for fresh groundwater lenses in small strip islands with spatially variable recharge. *Water Resources Research*, *57*, e2020WR029497. https://doi.org/10.1029/2020WR029497

Underwood, M. R., Peterson, F. L., & Voss, C. I. (1992). Groundwater lens dynamics of atoll islands. *Water Resources Research*, *28*, 2889–2902. https://doi.org/10.1029/92wr01723

UN-OHRLLS. (2015). Small island developing states in numbers: Climate change edition. In *Office of the high Representative for the Least developed Countries, Landlocked developing Countries and small island developing states*. Retrieved from https://sustainabledevelopment.un.org/content/documents/2189SIDS-IN-NUMBERS-CLIMATE-CHANGE-EDITION_2015.pdf

Vacher, H. L. (1988). Dupuit-Ghyben-Herzberg analysis of strip-island lenses, *Geological Society of America Bulletin*, *100*(4), 580–591. https://doi.org/10.1130/0016-7606(1988)100<0580:DGHAOS>2.3.CO;2

Voss, C. I., & Souza, W. R. (1987). Variable density flow and solute transport simulation of regional aquifers containing a narrow freshwater-saltwater transition zone. *Water Resources Research*, *23*, 1851–1866. https://doi.org/10.1029/WR023i010p01851

Werner, A. D., Jakovovic, D., & Simmons, C. T. (2009). Experimental observations of saltwater up-coning, *Journal of Hydrology*, *373*(1–2), 230–241. https://doi.org/10.1016/j.jhydrol.2009.05.004

Werner, A. D., Sharp, H. K., Galvis, S. C., Post, V. E. A., & Sinclair, P. (2017). Hydrogeology and management of freshwater lenses on atoll islands: Review of current knowledge and research needs, *Journal of Hydrology*, *551*, 819–844. https://doi.org/10.1016/j.jhydrol.2017.02.047

Yan, M., Lu, C., Werner, A. D., & Luo, J. (2021). Analytical, experimental, and numerical investigation of partially penetrating barriers for expanding island freshwater lenses. *Water Resources Research*, *57*, e2020WR028386. https://doi.org/10.1029/2020WR028386

Yao, Y., Andrews, C., Zheng, Y., He, X., Babovic, V., & Zheng, C. (2019). Development of fresh groundwater lens in coastal reclaimed islands, *Journal of Hydrology*, *573*, 365–375. https://doi.org/10.1016/j.jhydrol.2019.03.062

Zhang, J., Lu, C., & Werner, A. D. (2021). Analytical and experimental investigation of the impact of land reclamation on steady-state seawater extent in coastal aquifers. *Water Resources Research*, *57*, e2020WR029028. https://doi.org/10.1029/2020WR029028

Zhou, C., He, L., Yang, Q., & Fang, Z. (2010). Three-dimensional numerical simulation of freshwater lens in coral islands, *Journal of Hydraulic Engineering*, *41*(5), 560–566.

Zhou, C., Yang, Q., Fang, Z., Liang, H., & Wang, H. (2009). Numerical simulation of upconing and freshwater lens breakage in a coral island. In *Numerical simulation of upconing and freshwater lens breakage in a coral island* (pp. 154–159), Springer Berlin Heidelberg. https://doi.org/10.1007/978-3-540-89465-0_29